

AD-A131 949

ELECTRON BEAM TRAJECTORY IN A PHOTOMETER FIELD OF VIEW

1/1

(U) AIR FORCE GEOPHYSICS LAB HANSCOM AFB MA

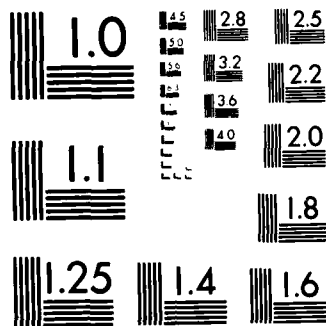
S T LAI ET AL. 16 FEB 83 AFGL-TR-83-0045

UNCLASSIFIED

F/G 12/1

NL





MICROCOPY RESOLUTION TEST CHART
NATIONAL BUREAU OF STANDARDS-1963-A

AD A131949

AFGL-TR-83-0045
ENVIRONMENTAL RESEARCH PAPERS, NO. 824



12

Electron Beam Trajectory in a Photometer Field of View

SHU T. LAI
H. A. COHEN

16 February 1983

DTIC
ELECTE
AUG 31 1983
S B

Approved for public release; distribution unlimited.

SPACE PHYSICS DIVISION PROJECT 7661
AIR FORCE GEOPHYSICS LABORATORY
HANSCOM AFB, MASSACHUSETTS 01731

AIR FORCE SYSTEMS COMMAND, USAF

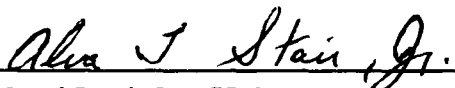


DTIC FILE COPY

83 08 25 060

This report has been reviewed by the ESD Public Affairs Office (PA)
and is releasable to the National Technical Information Service (NTIS).

This technical report has been reviewed and
is approved for publication.


DR. ALVA T. STAIR, Jr
Chief Scientist

Qualified requestors may obtain additional copies from the
Defense Technical Information Center. All others should apply
to the National Technical Information Service.

25517 25518 25519 25520 25521 25522 25523 25524 25525 25526 25527 25528 25529 25530 25531 25532 25533 25534 25535 25536 25537 25538 25539 25540 25541 25542 25543 25544 25545 25546 25547 25548 25549 25550 25551 25552 25553 25554 25555 25556 25557 25558 25559 25560 25561 25562 25563 25564 25565 25566 25567 25568 25569 25570 25571 25572 25573 25574 25575 25576 25577 25578 25579 25580 25581 25582 25583 25584 25585 25586 25587 25588 25589 25590 25591 25592 25593 25594 25595 25596 25597 25598 25599 25600 25601 25602 25603 25604 25605 25606 25607 25608 25609 25610 25611 25612 25613 25614 25615 25616 25617 25618 25619 25620 25621 25622 25623 25624 25625 25626 25627 25628 25629 25630 25631 25632 25633 25634 25635 25636 25637 25638 25639 25640 25641 25642 25643 25644 25645 25646 25647 25648 25649 25650 25651 25652 25653 25654 25655 25656 25657 25658 25659 25660 25661 25662 25663 25664 25665 25666 25667 25668 25669 25670 25671 25672 25673 25674 25675 25676 25677 25678 25679 25680 25681 25682 25683 25684 25685 25686 25687 25688 25689 25690 25691 25692 25693 25694 25695 25696 25697 25698 25699 25700 25701 25702 25703 25704 25705 25706 25707 25708 25709 25710 25711 25712 25713 25714 25715 25716 25717 25718 25719 25720 25721 25722 25723 25724 25725 25726 25727 25728 25729 25730 25731 25732 25733 25734 25735 25736 25737 25738 25739 25740 25741 25742 25743 25744 25745 25746 25747 25748 25749 25750 25751 25752 25753 25754 25755 25756 25757 25758 25759 25760 25761 25762 25763 25764 25765 25766 25767 25768 25769 25770 25771 25772 25773 25774 25775 25776 25777 25778 25779 25780 25781 25782 25783 25784 25785 25786 25787 25788 25789 25790 25791 25792 25793 25794 25795 25796 25797 25798 25799 25800 25801 25802 25803 25804 25805 25806 25807 25808 25809 25810 25811 25812 25813 25814 25815 25816 25817 25818 25819 25820 25821 25822 25823 25824 25825 25826 25827 25828 25829 25830 25831 25832 25833 25834 25835 25836 25837 25838 25839 25840 25841 25842 25843 25844 25845 25846 25847 25848 25849 25850 25851 25852 25853 25854 25855 25856 25857 25858 25859 25860 25861 25862 25863 25864 25865 25866 25867 25868 25869 25870 25871 25872 25873 25874 25875 25876 25877 25878 25879 25880 25881 25882 25883 25884 25885 25886 25887 25888 25889 25890 25891 25892 25893 25894 25895 25896 25897 25898 25899 25900 25901 25902 25903 25904 25905 25906 25907 25908 25909 25910 25911 25912 25913 25914 25915 25916 25917 25918 25919 25920 25921 25922 25923 25924 25925 25926 25927 25928 25929 25930 25931 25932 25933 25934 25935 25936 25937 25938 25939 25940 25941 25942 25943 25944 25945 25946 25947 25948 25949 25950 25951 25952 25953 25954 25955 25956 25957 25958 25959 25960 25961 25962 25963 25964 25965 25966 25967 25968 25969 25970 25971 25972 25973 25974 25975 25976 25977 25978 25979 25980 25981 25982 25983 25984 25985 25986 25987 25988 25989 25990 25991 25992 25993 25994 25995 25996 25997 25998 25999 26000 26001 26002 26003 26004 26005 26006 26007 26008 26009 26010 26011 26012 26013 26014 26015 26016 26017 26018 26019 26020 26021 26022 26023 26024 26025 26026 26027 26028 26029 26030 26031 26032 26033 26034 26035 26036 26037 26038 26039 26040 26041 26042 26043 26044 26045 26046 26047 26048 26049 26050 26051 26052 26053 26054 26055 26056 26057 26058 26059 26060 26061 26062 26063 26064 26065 26066 26067 26068 26069 26070 26071 26072 26073 26074 26075 26076 26077 26078 26079 26080 26081 26082 26083 26084 26085 26086 26087 26088 26089 26090 26091 26092 26093 26094 26095 26096 26097 26098 26099 26100 26101 26102 26103 26104 26105 26106 26107 26108 26109 26110 26111 26112 26113 26114 26115 26116 26117 26118 26119 26120 26121 26122 26123 26124 26125 26126 26127 26128 26129 26130 26131 26132 26133 26134 26135 26136 26137 26138 26139 26140 26141 26142 26143 26144 26145 26146 26147 26148 26149 26150 26151 26152 26153 26154 26155 26156 26157 26158 26159 26160 26161 26162 26163 26164 26165 26166 26167 26168 26169 26170 26171 26172 26173 26174 26175 26176 26177 26178 26179 26180 26181 26182 26183 26184 26185 26186 26187 26188 26189 26190 26191 26192 26193 26194 26195 26196 26197 26198 26

[illegible]

Contents

| | |
|--|----|
| 1. INTRODUCTION | 5 |
| 2. GEOMETRY OF INSTRUMENTATION | 6 |
| 3. ELECTRON TRAJECTORY—B COORDINATE SYSTEM | 8 |
| 4. ELECTRON TRAJECTORY—R COORDINATE SYSTEM | 9 |
| 5. LUMINOSITY | 10 |
| 6. SCEN ROCKET | 13 |
| APPENDIX A: Blockage of Field-of-View by the Horizon | 17 |

Illustrations

| | |
|--|----|
| 1. Geometry of Electron Gun G and Photometer P Mounted on a Section of the Rocket Body | 6 |
| 2. Geometry of Electron Gun G and Photometer P at Any Instant of Time | 7 |
| 3. Circular Angular Field-of-View of Photometer | 7 |
| 4. B Coordinate System | 8 |
| 5. R Coordinate System | 9 |
| 6. Typical Behavior of Function $F(t)$ | 11 |
| 7. Electron Beam Trajectory in Photometer Field-of-View | 11 |

Illustrations

| | | |
|-----|--|----|
| 8. | Circular Electron Trajectory When Initial Beam Velocity is Perpendicular to the Magnetic Field | 12 |
| 9. | Loci of Non-propagation Mode as a Function of Pitch Angle and Azimuth Angle | 14 |
| 10. | Computer Simulation of Electron Beam Trajectory as Viewed at the Photometer on the SCEX Rocket, the Magnetic Field Look-angle in This Simulation is at (0°, 25°) | 14 |
| 11. | Computer Simulation of Electron Beam Trajectory as Viewed at the Photometer on the SCEX Rocket, the Magnetic Field Look-angle in This Simulation is at (0°, 40°) | 15 |
| 12. | Geometrical Factor of Luminosity of the Electron Beam as Viewed by the Photometer on the SCEX Rocket, Beam Energy is 1900 eV | 15 |
| 13. | Geometrical Factor of Luminosity of the Electron Beam as Viewed by the Photometer on the SCEX Rocket, Beam Energy is 8000 eV | 16 |
| 14. | Comparison of the Geometrical Factors for the Cases of 1900-eV and 8000-eV Beam Energies | 16 |
| A1. | Blockage of Photometer Field-of-View by the Horizon | 17 |
| A2. | Solution of the Maximum Angle β_{\max} | 18 |

Tables

| | | |
|----|--------------------------------|----|
| 1. | SCEX Photometer Specifications | 13 |
|----|--------------------------------|----|

| | |
|--------------------|-------------------------------------|
| Accession No. | |
| NTIS G342 | <input checked="" type="checkbox"/> |
| DTIC TAB | <input type="checkbox"/> |
| Unannounced | <input type="checkbox"/> |
| Justification | |
| By _____ | |
| Distribution/ | |
| Availability Codes | |
| Dist | Avail and/or Special |
| A | |



Electron Beam Trajectory in a Photometer Field of View

1. INTRODUCTION

From the inception of the use of electron beams on sounding rocket flights, photometers have been used to measure the light produced by the interaction of the electron beams with the gas surrounding the rocket payload.^{1,2} Since the path of an electron is affected by the earth's magnetic field, the measurable, the luminosity of the beam-gas interaction in the field-of-view of the photometer is also similarly affected. Early experiments tried to minimize these effects by making measurements close to the payload and with a restricted field-of-view for the photometer. For measurements away from the vehicle, and for wide viewing angles, explicit calculations of particle trajectory in the field-of-view of optical devices are necessary for the planning and interpretation of experiments.

Received for publication 14 February 1969

1. J. De Boer, *J. High Speed Physics*, **W. B. R.**, (1969) Small Rocket Instrumentation, Dordrecht, North Holland Publishing Co., Amsterdam, Holland.

2. J. De Boer, J. H. van der Horst, and J. A. van der Horst, *Journal of Space Research*, **1**, 1 (1969).
3. J. De Boer, *Journal of Space Research*, **1**, 1 (1969).

2. GEOMETRY OF INSTRUMENTATION

A schematic diagram of the geometry of the instrumentation is shown in Figure 1. The photometer is placed on a section of the rocket body at a distance d from the gun. The photometer is assumed to be at a distance d from the gun, and is offset at an angle β from the gun's axis. The angle β is assumed to be small so that blockage of the photometer view by the rocket surface does not occur. (See Appendix A.)

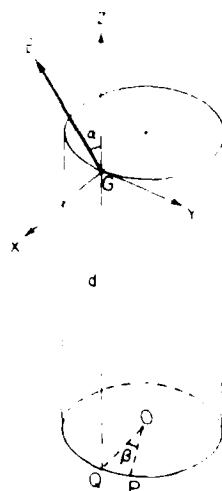


Figure 1. Geometry of Electron Gun G and Photometer P Mounted on a Section of the Rocket Body. The origin of the coordinate system is at G, the z-distance from the gun to the photometer is d .

In the x, y, z coordinate system shown in Figure 1, the gun G is located at the origin. The photometer P is mounted at $- \rho + \rho \cos \beta, \rho \sin \beta, -d$. At any time t , let a beam electron be located at x, y, z . It subtends angles θ_x and θ_y at the photometer:

$$\theta_x = \tan^{-1} \left(\frac{x + \rho - \rho \cos \beta}{z + d} \right), \quad (1)$$

$$\theta_y = \tan^{-1} \left(\frac{y - \rho \sin \beta}{z + d} \right). \quad (2)$$

In the special case $\beta = 0$, the photometer would be located directly below G at distance d , (see Figure 2).

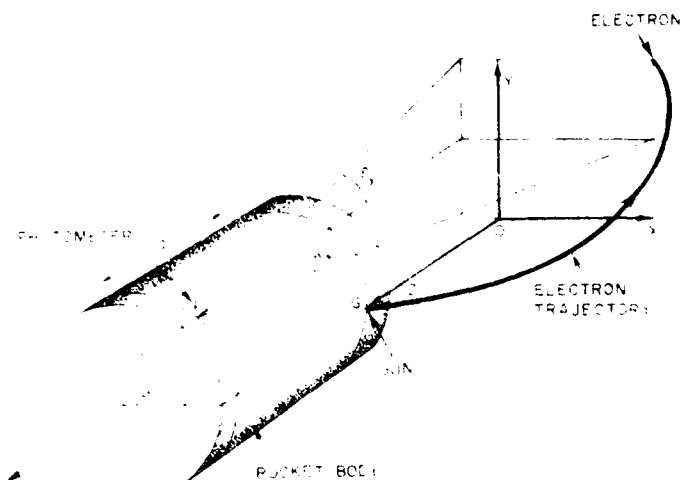


Figure 2. Geometry of Electron Gun G and Photometer P at Any Instant of Time. Beam electron subtends angles θ_x and θ_y at Photometer P.

The field-of-view of the photometer is designed to be limited. It is assumed that the field is circular with the center at $\theta_x(c)$ and $\theta_y(c)$ and radius θ_p . An electron at $\theta_x(t)$, $\theta_y(t)$, would be in the photometer field-of-view if

$$[\theta_x(t) - \theta_x(c)]^2 + [\theta_y(t) - \theta_y(c)]^2 \leq \theta_p^2. \quad (6)$$

If the above inequality is not satisfied, the electron is outside the photometer field-of-view, as in Figure 3.

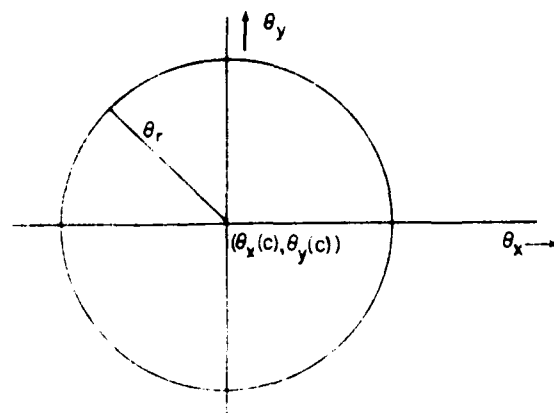


Figure 3. Circular Angular Field-of-View of Photometer.

3. ELECTRON TRAJECTORY-B COORDINATE SYSTEM

The luminosity of the beam atmosphere interaction measured in the photometer's field-of-view is sensitive to the magnetic field orientation with respect to the beam or rocket. Part of the electron trajectory may move in or out of the field-of-view.

In the B system of coordinates as defined in Figure 4, the magnetic field \vec{B} is parallel to the z axis. The vector \vec{V} is the initial beam velocity. The v axis is defined as along $\vec{z} \times \vec{V}$. Thus, \vec{V} lies in the z-x plane. The origin of the beam is at $x=0$, $y=0$, $z=0$. The equation of motion of a beam in the B system is as follows:

$$\begin{bmatrix} x(t) \\ y(t) \\ z(t) \end{bmatrix}_B = \begin{bmatrix} R \sin \omega t \\ R - R \cos \omega t \\ V_{||} t \end{bmatrix} \quad (4)$$

where

$$\omega = \frac{eB}{mc}$$

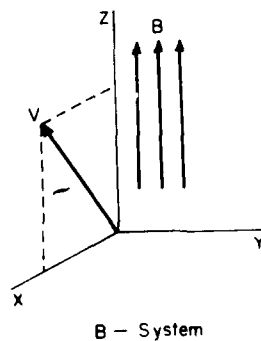


Figure 4. B-Coordinate System. Magnetic field \vec{B} is defined along z-axis

and

$$R = \frac{V_{\perp}}{\omega}$$

where R is gyroradius, ω is gyrofrequency, t is time, and V_{\parallel} and V_{\perp} are the velocity component parallel and perpendicular to the magnetic field respectively. The energy E of the electron is related to the velocity V by $E = 1/2 m V^2$, where m is the mass of electron.

In the B system, the \vec{B} vector is fixed, the \vec{V} vector varies but lies in the z - x plane, and, as the rocket spins, the photometer look-angle varies with time.

4. ELECTRON TRAJECTORY-R COORDINATE SYSTEM

In order to study the electron trajectory in the field-of-view of the photometer, it is more convenient to define an R system of coordinates in which the photometer look-angle is always fixed and the \vec{B} vector varies with time. In the R system (see Figure 5), the z axis is defined as parallel to the rocket axis, y axis is in radial direction, and x completes the right-handed system.

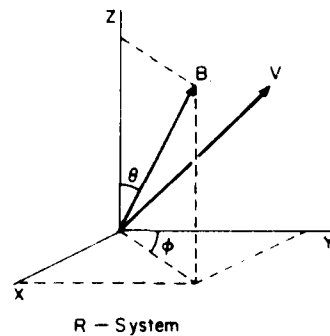


Figure 5. R Coordinate System. The z -axis is parallel to rocket body axis. This is the same coordinate system used in Figure 1.

At time t , let the magnetic field vector \vec{B} be in arbitrary direction, defined by pitch angle $\theta(t)$ and azimuth angle $\phi(t)$ in the R system (see Figure 5).

The equation of motion of a beam electron is obtained in the R system by an orthogonal transformation from Eq. (4) in the B system.

$$\begin{bmatrix} x(t) \\ y(t) \\ z(t) \end{bmatrix}_R = \begin{bmatrix} m_1 & m_2 & m_3 \\ n_1 & n_2 & n_3 \\ p_1 & p_2 & p_3 \end{bmatrix} \begin{bmatrix} x(t) \\ y(t) \\ z(t) \end{bmatrix}_B \quad (5)$$

where m_i , n_i , p_i are the direction cosines of the i -th basis vector of the R system w.r.t. the B system.

In terms of cross products, the transformation equation is as follows:

$$\begin{bmatrix} x(t) \\ y(t) \\ z(t) \end{bmatrix}_R = \begin{bmatrix} (\vec{B} \cdot \vec{V}) \cdot \vec{B} - 1(\vec{B} \cdot \vec{V}) \cdot \vec{B} \\ \vec{B} \cdot \vec{V} \cdot \vec{B} \cdot \vec{V} \\ \vec{B} \cdot \vec{B} \end{bmatrix} \begin{bmatrix} x(t) \\ y(t) \\ z(t) \end{bmatrix}_B \quad (6)$$

In the special case when the magnetic field \vec{B} lies in the plane of the initial electron beam direction and the rocket axis, the transformation equation becomes

$$\begin{bmatrix} x(t) \\ y(t) \\ z(t) \end{bmatrix}_R = \begin{bmatrix} 0 & 1 & 0 \\ -\cos \theta & 0 & \sin \theta \\ \sin \theta & 0 & \cos \theta \end{bmatrix} \begin{bmatrix} x(t) \\ y(t) \\ z(t) \end{bmatrix}_B \quad (7)$$

where

$$\frac{\vec{B}}{B} = (0, \cos \theta, \sin \theta).$$

5. LUMINOSITY

The angular coordinates θ_x and θ_y of an electron as viewed by the photometer are given by Eqs. (1) and (2).

Using the orthogonal transformation equation, Eq. (4), one can write down the angular coordinates (Figure 2), as viewed by a photometer lying at $(0, 0, -d)$:

$$\begin{aligned} \theta_x(t) &= \tan^{-1} \left(\frac{x(t) \cdot \rho - \rho \cos \beta}{z(t) + d} \right) \\ \theta_y(t) &= \tan^{-1} \left(\frac{y(t) - \rho \sin \beta}{z(t) + d} \right) \end{aligned} \quad (8)$$

The electron would lie in the photometer field-of-view if Eq. (3) is satisfied (see Figure 3). Equivalently, let us define a function $F(t)$:

$$F(t) = \frac{1}{r^2} = \frac{1}{r^2} \left\{ [x_X(t) - x_X(c)]^2 + [y_V(t) - y_V(c)]^2 \right\}.$$

If Eq. (3) is satisfied, then the function $F(t)$ is positive, (see Figures 6 and 7).

$$F(t) > 0. \quad (9)$$

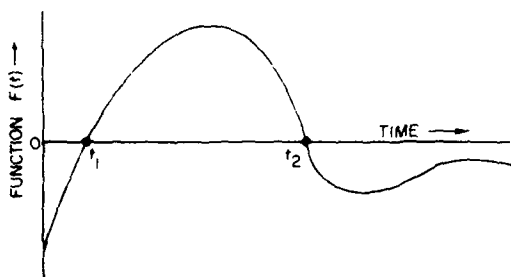


Figure 6. Typical Behavior of Function $F(t)$. The beam electron is in the photometer field-of-view during the period t_1 to t_2 .

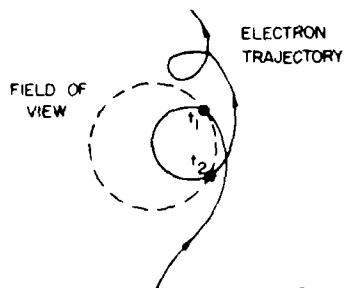


Figure 7. Electron Beam Trajectory in Photometer Field-of-View. The beam entering field-of-view (dashed circle) at t_1 and leaves at t_2 .

If the electron interacts with a gas atom, or molecule, to create ionization or excitation, the luminosity $L(E)$ measured at the photometer is proportional to the inverse square of the distance $s(t)$ of the electron from the photometer.

$$L(t) = N \int_{t_1}^{t_2} L(E) \frac{1}{s^2(t)} dt \quad (10)$$

$$L(t) = N \int_{t_1}^{t_2} L(E) \frac{1}{s^2(t)} dt$$

where N is a proportionality constant, V is the velocity of the electron, and $\sigma(E)$ is the cross-section of ionization and excitation. It is assumed that no significant energy loss ($\Delta E/E \ll 1$) takes place along the beam while in the photometer field-of-view. $\mathbb{H}(x)$ is a step function:

$$\mathbb{H}(x) = \begin{cases} 1 & \text{if } x > 0 \\ 0 & \text{if } x \leq 0 \end{cases}.$$

From Eq. (10), one obtains the geometric factor G as follows:

$$L(E) = N V(E) \sigma(E) G$$

where

$$G = \sum_{i=1}^{\infty} \int_{t_{2i-1}}^{t_{2i}} dt \frac{1}{s^2(t)}$$

$$s(t) = [x^2(t) + v^2(t) + (z + d)^2]^{1/2}.$$

When the initial velocity vector \vec{V} of the electron is perpendicular to the magnetic field vector \vec{B} , the beam forms a circular path. The condition is

$$\vec{B} \cdot \vec{V} = 0. \quad (11)$$

Every electron injected into the path would stay in the path and never propagate away (see Figure 8). This is a nonpropagation mode. The luminosity $L(E)$ for this mode is high, because $s^{-2}(t)$ does not decrease with time.

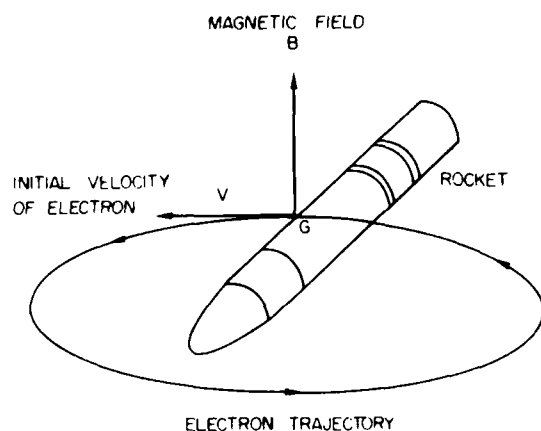


Figure 8. Circular Electron Trajectory When Initial Electron Velocity is Perpendicular to the Magnetic Field

The above condition agrees with the experimental result of Israelson and Winckler³ who detected a substantial increase in photon flux at 90° pitch angle in the Echo 2 rocket beam experiment.

6. SCEx ROCKET

As an example, for the SCEx rocket^{*} experiment the specifications of the photometer on-board is given in Table 1.

Table 1. SCEx Photometer Specifications

| | |
|---|-------------|
| Photometer rotation angle β | = 0° |
| Photometer distance from gun (d) | = 119 cm |
| Center of field-of-view [$\theta_x(c)$, $\theta_y(c)$] | = [0°, 20°] |
| Radius of field-of-view θ_r | = 15° |

The condition of Eq. (11) for nonpropagation modes to exist becomes

$$\sin \theta \cos \phi + \cos \theta = 0 \quad (12)$$

where θ and ϕ are rocket pitch and azimuth angles. The solutions of Eq. (12) are plotted in Figure 9.

In Figure 9, the pitch angle actually runs only from 0° to 180° because it is a cone angle. The azimuth angle ϕ at 180° is the same as -180° because it is a rotation angle. Solutions exist only for a range of values of pitch angle.

Examples of electron beam trajectories as viewed at the SCEx photometer are presented in Figures 10 and 11. Three-dimensional plots of luminosity, for the case of SCEx, as a function of θ and ϕ , are shown in Figures 12 and 13. The location of the spikes should fall on a continuous curve given in Eq. (12) (Figure 9) but computer calculation requires the use of grid points which are discrete. Therefore the singularities do not look like a continuous wall, but appear as spikes. The 1900-eV case gives a generally higher (about 2 to 3 times) luminosity than the

3. Israelson, G., and Winckler, J.R. (1975) Measurement of 3914-Å light production and electron scattering from electron beams artificially injected into the ionosphere, J. Geophys. Res. 80:No. 25:3709-3712.

* NASA Rocket 27,045, launched on 27 January 1982, from Churchill, Canada.

4000-ew, and give the following equations that show that the electron beam is in focus:

Electron beam diameter at 1000 ft = $1000 \times \frac{1}{1000} = 1$ ft. (1000 ft. is the distance from the SCEN Rocket to the photometer, and 1000 is the magnification factor.)

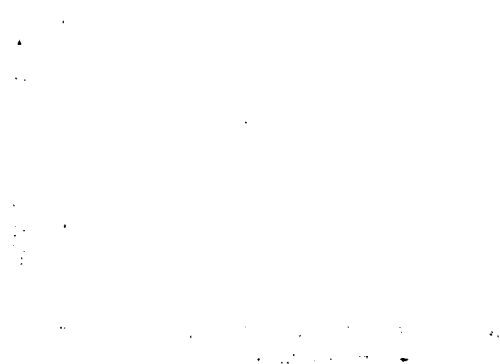


Figure 9. Plot of Normalization Mode as a function of Pitch Angle and Azimuth Angle

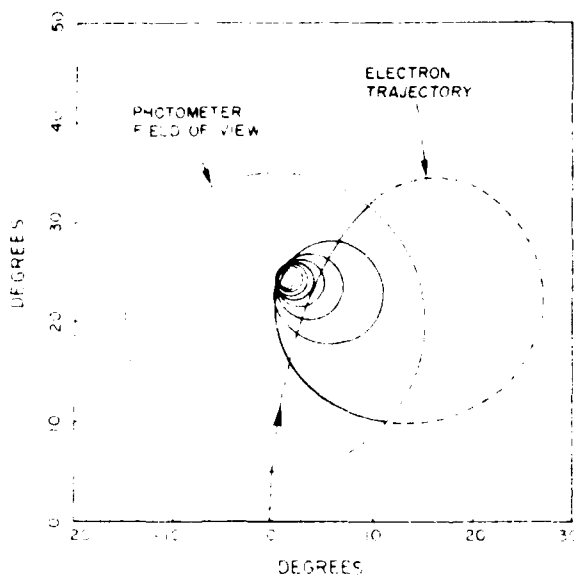


Figure 10. Computer Simulation of Electron Beam Trajectory as Viewed at the Photometer on the SCEN Rocket, the Magnetic Field Look-angle in This Simulation is 0°, 25°. The dashed part of the trajectory is outside the circular field of view.

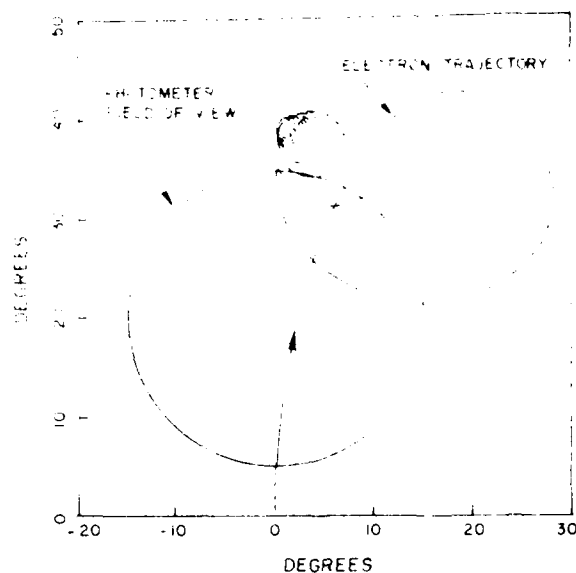


Figure 11. Electron Trajectory as Viewed by the SC/EX Rocket Photometer at 1000 eV. However, the Maximum Electron Angle is 100 degrees. Simulation is at 40 degrees. The dashed part of the trajectory is outside the photometer field of view.

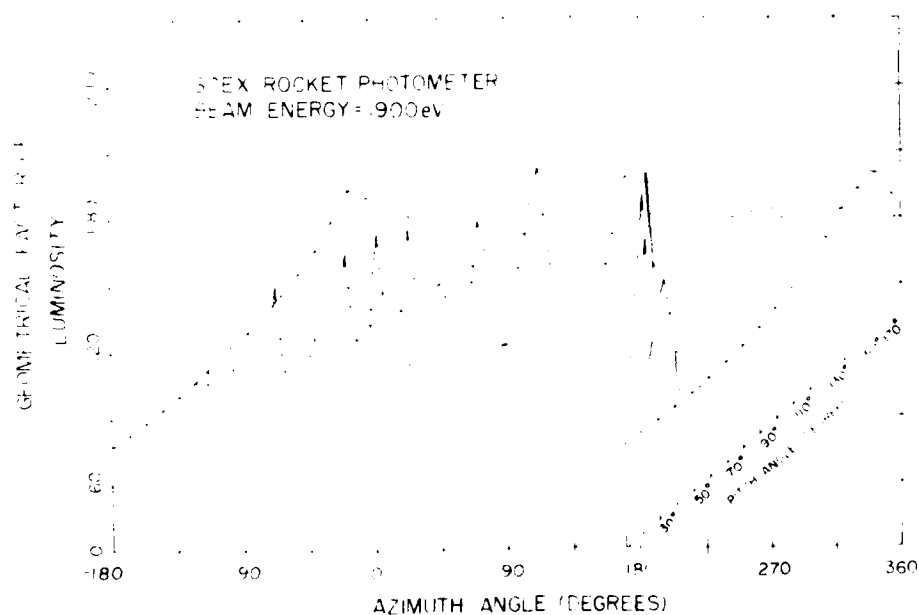


Figure 12. Geometrical Factor of Luminosity of the Electron Beam as Viewed by the Photometer on the SC/EX Rocket, Beam Energy is 1900 eV. The functional dependence on pitch and azimuth angles are plotted

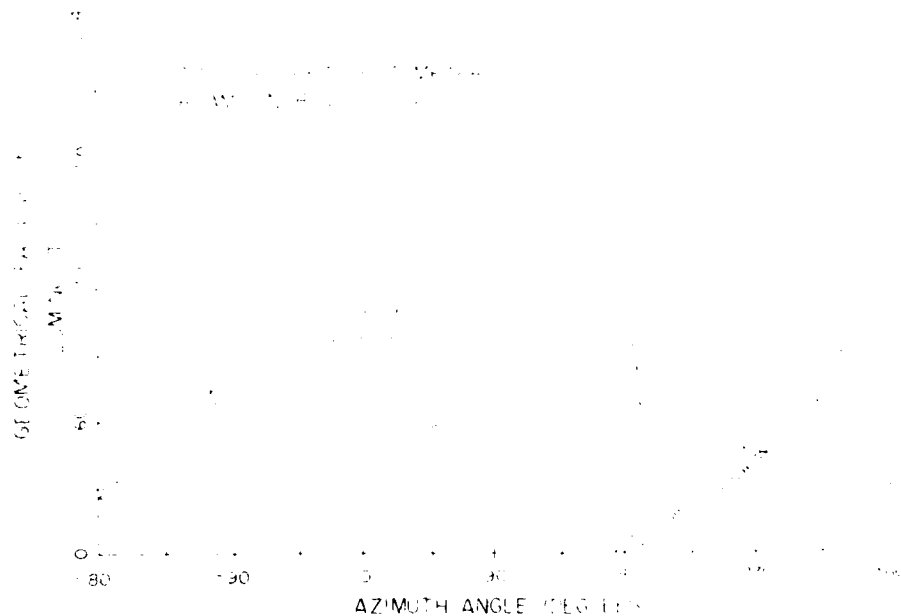


Figure 13. Geometrical Factor of Luminosity of the Electron Beam as Viewed by the Photometer on the SCEN Rocket. Beam Energy is 8000 eV. The functional dependence on pitch and azimuth angles are plotted.

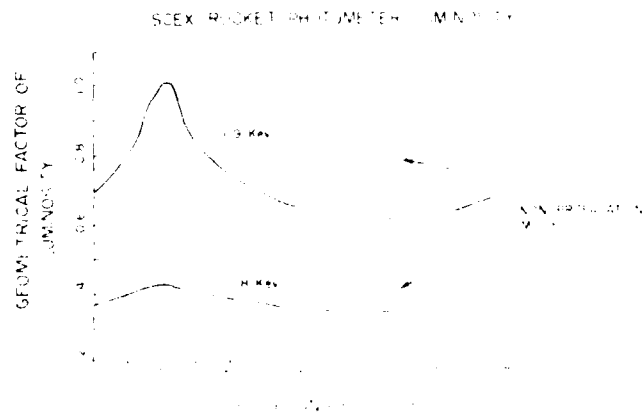


Figure 14. Comparison of the Geometrical Factor of Luminosity of the Electron Beam as Viewed by the SCEN Rocket. Beam Energy is 1000 eV and 8000 eV. Beam Energy is 1000 eV and 8000 eV. Beam Energy is 1000 eV and 8000 eV. Beam Energy is 1000 eV and 8000 eV.

Appendix A

Blockage of Field-of-View by the Horizon

The blockage of the field-of-view, for a wide angle photometer P, is determined by the horizon. For the geometry shown in Figure A1, the equation of the horizon is

$$y = mx + c,$$

where

$$m = -\tan \beta$$

$$c = \rho(\sec \beta - 1).$$

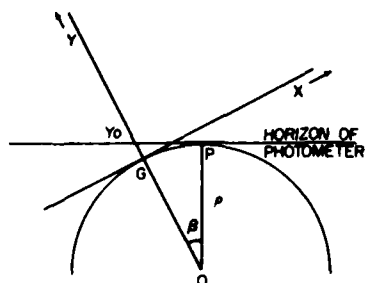


Figure A1. Blockage of Photometer Field-of-View by the Horizon

If at $x = 0$, blockage is desired to be below y_0 , then

$$\rho(\sec \beta - 1) < y_0,$$

that is

$$\frac{1}{\cos \beta} < \frac{y_0 + \rho}{\rho}.$$

This determines the maximum β , (see Figure A2).

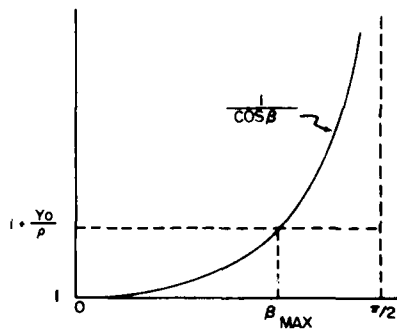


Figure A2. Solution of
the Maximum Angle
 β_{max}

END

FILMED

9-83

DTIC